Available online at www.sciencedirect.com

ScienceDirect

Procedia Engineering 10 (2011) 746–751

Engineering Procedia

ICM11

Application of a failure assessment diagram under rolling contact to components with hardness variable along the depth

G. Donzella[a], C. Petrogalli[a] and A. Mazzù[a*]

[a] *University of Brescia, Department of Mechanical and Industrial Engineering, via Branze, 38, 25123 Brescia – Italy*

Abstract

A development of a failure assessment diagram for the evaluation of the safe working area of components subjected to rolling contact loading is here presented regarding the application to components whose hardness varies along the depth. The approach takes into account the influence of inherent defects in determining subsurface rolling contact fatigue, depending on working conditions, material properties and hardness profile along the depth. For this aim, crack propagation from inherent defects is assessed in terms of applied stress intensity factor range normalized with respect to short crack growth threshold, defect – free fatigue is assessed in terms of Dang Van stress normalized with respect to shear fatigue limit, where the material quantities depend on hardness variable with depth. These two normalized quantities are the coordinates of the points of a "reference curve" in the failure assessment diagram, which location indicates whether and where failure is expected to occur. By analysing different combinations of loading condition, inclusion dimension and hardness profile, it was possible obtaining a design diagram of general validity, which allows a fast prediction of safety against subsurface rolling contact fatigue.

Keywords: Rolling contact fatigue, failure assessment diagram, surface hardened components

1. Introduction

Components subjected to rolling contact loading and having a variable hardness along the depth are common in industrial applications: gears, cams, bearing are some examples of them. The hardened layer is usually obtained by heat or mechanical treatments, addressing the requirement of high surface resistance, especially to wear, which is one of the damage processes more afflicting these components. While surface hardness is usually quite easy to be specified in the design phase, the definition of the optimum hardness profile remains a matter of discussion, depending it on both working conditions and

*Corresponding author. Tel.: +39 030 371 5525; fax: +39 030 371 5942
E-mail address: angelo.mazzu@ing.unibs.it

1877–7058 © 2011 Published by Elsevier Ltd.
doi:10.1016/j.proeng.2011.04.124

material mechanical and micro-structural properties [1], [2]. The prediction of rolling contact loading resistance of these components is a complex problem and a comprehensive approach for this aim is not available yet, due to the difficulty in taking into account the numerous parameters involved. In addition, different damage mechanisms can act on these components, being mainly imputable to surface or sub-surface rolling contact fatigue (RCF) [3]. In this work, an approach to specifically evaluate the effect of different hardness profiles on the subsurface originated RCF is developed. For this aim, a previously proposed failure assessment diagram (FAD) for rolling contact loading [4] has been generalised considering material properties varying along the depth. The FAD takes explicitly into account the effect of inclusions, considering them as equivalent early formed cracks and defining the RCF limit in terms of propagation threshold. This feature is particularly important for hard components, as they are very sensitive to micro-structural defects and their RCF resistance is strongly related to material cleanliness [5]. According to this approach, the risk of RCF failure can be evaluated by plotting a reference curve on the FAD and evaluating a correspondent safety factor. This procedure has been used for analysing different cases, varying contact pressure, inclusion dimension and hardness profile. The results of these analyses have been synthesized in a graph which indicates in a normalized way the limit contact pressure as a function of the other parameters, thus constituting a useful design tool.

2. Extension of the FAD for rolling contact loading to the case of hardness varying with depth

The FAD for components subjected to rolling contact, recently proposed in [4], considers fatigue limit as "non propagation" condition of inherent short cracks, assumed present in the component following the Murakami theory [6] and having a size equal to that of the maximum inclusion expected in the layer interested by the Herztian stress field, determined by the statistics of extreme values. The approach is based on the El-Haddad model [7], by which the short cracks threshold is expressed in the form:

$$\Delta K_{th} = \Delta K_{th\ l.c.} \cdot \sqrt{a/(a + a_D)} \tag{1}$$

where ΔK_{th} and $\Delta K_{th\,l.c.}$ are respectively the short and long crack growth thresholds and a_D is the critical crack length [8]. Also considering that for rolling contact loading the SIF range during a contact cycle can be expressed as a function of the applied Hertzian pressure p, we can define:

$$\Delta K = y p \sqrt{\pi a} \tag{2}$$

$$\begin{cases} P_p = p_{cr}/p_o \\ K_P = \Delta K_{th}/\Delta K_{th\,l.c.} \end{cases} \tag{3}$$

where p_{cr} and p_o are respectively the RCF pressure limit in presence of a crack with length "a" and for a plain specimen (without defects influence), the FAD is described by the equation:

$$K_p = \sqrt{1 - P_p^2} \tag{4}$$

An alternative way to define P_p is to use the Dang Van criterion [9], which has extensively applied to rolling contact problems [10], [11]. Following this criterion, an equivalent Dang Van stress is defined by the formula:

$$\sigma_{D.V.} = \max_t \left[\tau_{max}(t) + a_{D.V.} \cdot \sigma_H(t)\right] \tag{5}$$

The limit condition. i.e fatigue occurrence, happens if $\boldsymbol{\sigma_{D.V.} = \Delta\tau_0}$, where $\boldsymbol{\Delta\tau_0}$ is the reversed torsion fatigue limit for a defect-free material (single amplitude). The Dang Van parameter a_{DV} takes into account the effect of the hydrostatic stress. It has however shown by Desimone and co-workers [10] that the criterion is highly under-conservative for a compressive hydrostatic stress, as happens in rolling contact loading, being in particular not acceptable to represent the limit curve $\tau_{max}(t)$-$\sigma_H(t)$ as a single straight line. A modification of the criterion should be therefore applied for RCF, considering a_{DV}=0.
Under this assumption, $\sigma_{D.V.}$ does not depend on residual stresses, which enter in the hydrostatic stress, and is therefore proportional to the applied pressure, so that eq. (3) can be also written in the form:

$$\begin{cases} P_p = \sigma_{D.V.cr} / \Delta\tau_0 \,, \\ K_P = \Delta K_{th} / \Delta K_{th\,l.c.} \end{cases} \tag{6}$$

which is more suitable for studying components with hardness variable along the depth.
The relationship reported in eqs. (6) defines an arc of a circle and can be easily drawn on a graph, representing a limit curve for RCF (infinite life), as shown in fig.1a.

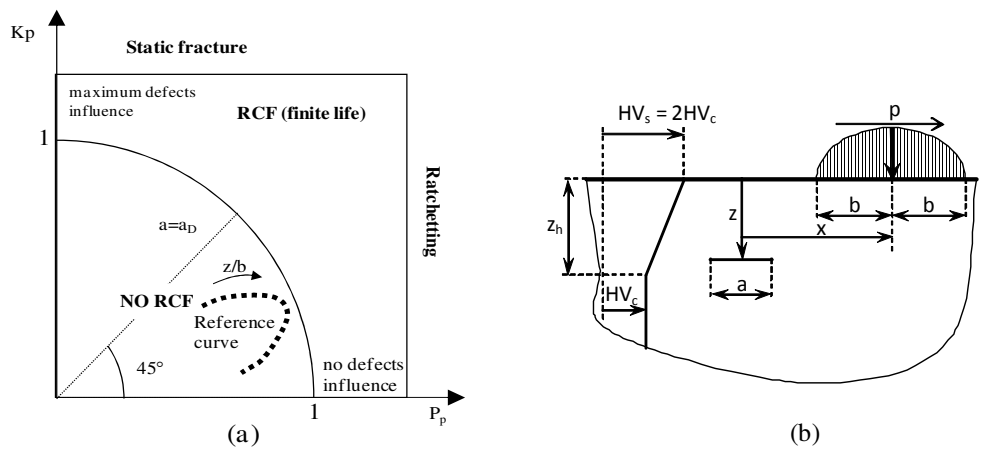

Fig.1 . (a) Scheme of the hardness profile and of the contact loading condition in a cracked material; (b) Failure assessment diagram for rolling contact loading

For the assessment, the reference point describing the working condition has to be reported on the graph. If the reference point falls under the limit curve, it means that the flawed component will no experience fatigue, otherwise inherent defects are predicted to be able to propagate determining RCF failure, i.e. a component finite life. Limitations to monotonic fracture and ratchetting can be added to this diagram by plotting an horizontal and a vertical straight line respectively passing for the normalised fracture toughness $K_{IC}(1\text{-}R) / \Delta K_{th\ l.c}$ and the normalised shakedown pressure p_{sh} / p_o. While for homogeneous material an unique reference point for subsurface RCF is determined at the most critical depth (which usually corresponds to that of the maximum orthogonal shear stress), in the case of components having hardness variable with depth, a series of references points, corresponding to different depths and forming a "reference curve", have to be determined in order to find the most dangerous location for RCF onset. The failure assessment is made in this case by comparing the reference curve with the RCF limitation curve, checking in particular way if some point of the reference curve touches or overcomes it (see fig.1a). For this aim, the threshold material quantities $\Delta\tau_0$ and $\Delta K_{th\ l.c.}$ have to be expressed as a function of hardness. For low alloy steels, the relationships described in the following can be useful.

The reversed torsion fatigue limit results well related to the uni-axial plain fatigue limit $\Delta\sigma_o$ throughout the von Mises criterion, and the best fit highlighted by Atzori et al [12]:

$$\Delta\tau_0 = \left(1/\sqrt{3}\right)\cdot\Delta\sigma_o \cong 0.274\cdot\sigma_{UTS} \tag{7}$$

while the ultimate stress and the long crack growth threshold can be determined respectively from the Roessle & Fatemi [13] and Kato's relationship [14]:

$$\sigma_{UTS} = 0.0012\cdot HB^2 + 3.3HB \tag{8}$$

$$\Delta K_{th\ l.c.R=0} = 2.45 + 3.41\cdot 10^{-3}\cdot HV \tag{9}$$

3. Applications

Different combinations of loading condition, inclusion dimension and hardness profile were studied with the above described FAD, in order to evaluate the effect on the subsurface RCF limit. Ratchetting has not been considered in this work, as it is not a common damage mechanism in surface hardened components. The problem is represented as a 2D elastic half space in plane strain condition, with a straight crack of length "a" at depth z in the subsurface region, parallel to the contact surface. The crack is supposed to propagate in coplanar mode II, according to many experimental evidences and numerical models of subsurface RCF in hardened components. A Hertz pressure distribution, characterized by maximum value p, half-width b, moves along the contact surface in x direction (see Fig. 1b). The hardness profile was simplified as varying linearly from the surface to the core, with a ratio of the surface to core hardness fixed to 2 (except for the uniform hardness case). The ratio of the hardened depth z_h to the contact area halfwidth b was 0.5, 0.8, 1, 1.5, 3 and infinite (corresponding to the uniform hardness case), where z_h is the thickness of the layer characterized by varying hardness. Obviously, many other hardness profiles can exist, but these are well representative of most common real cases. The material properties (in terms of fatigue limit and SIF threshold) were derived from these profiles according to equations (7), (8) and (9). The Dang Van shear stress was calculated by means of the Boussinesq-Cerruti method on a grid of nodes under the contact surface, extending from 0.1b to 1.9b along the z direction, and from -b to +b along the x direction. For each depth, the stress variation along x represents a load cycle. The applied stress intensity factor was calculated by numerical integration of the following expression:

$$K_{II} = \int_{-a/2}^{+a/2} h_{II}(x,z,a)\cdot\tau_{xz}(x,z)dx \tag{10}$$

where $h_{II}(x,z,a)$ is a weight function proposed by Mazzù [15] depending only on geometry, and $\tau_{xz}(x,z)$ is the orthogonal shear stress along the crack front, calculated as the crack was not present. The SIF calculation was carried out for cracks centered on the same node grid of the stress calculation, such that the K_{II} variation during a load cycle was obtained. The obtained SIF variation ΔK_{II} was divided by 2 because, as shown by Sakae et al. [16], friction between crack faces reduces drastically the applied SIF. In particular, it was found that a friction coefficient of 0.4 (a realistic value for this problem) reduces ΔK_{II} by the half. Each calculation was carried out in the limit condition, i.e. with $Sp^2 + Kp^2 = 1$ somewhere in the material; furthermore, for each value of z, a safety factor η was calculated as follows:

$$\eta = 1/\sqrt{P_P^2 + K_P^2} \tag{11}$$

In fig. 2a some results for pure rolling contact and uniform hardness are shown in terms of references curves for different values of $p/\Delta\tau_0$ and a/a_D. Each curve represents the variation of S_p and K_p along the

depth of a single case: the limit in any case is reached at the maximum τ_{xz} stress depth. As a/a_D increases, $p/\Delta\tau_0$ decreases, and the curves approach the region of the diagram where the maximum defect influence is expected. The increment of a/a_D is due either to the increment of the inherent defects dimension, or to the decrement of the a_D parameter, corresponding to an increment of the material defect sensitivity.

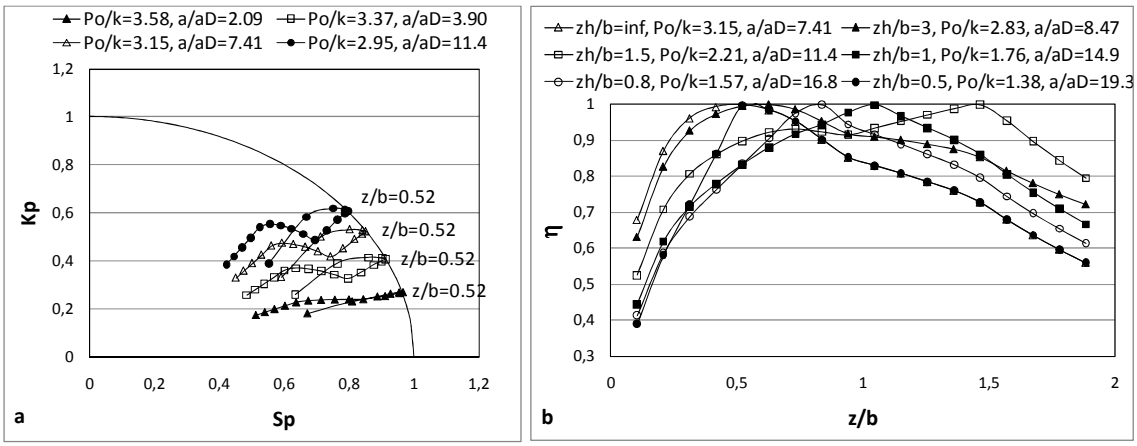

Fig.2 . (a) References curves for different combinations of contact loading and inclusion dimension, in the limit condition; (b) Plot of the safety factor along the depth of materials with different hardness profiles, in the limit condition

The effect of hardness profile is shown in fig. 2b in terms of safety factor η along the depth for frictionless contact. The $\Delta\tau_0$ and a_D values indicated in the legend are calculated on the basis of the surface (z = 0) material properties. The effect of a variable hardness is to move the critical point from the depth of maximum hertz stress (z/b=0.5) towards deeper layers, depending on the hardness profile. If the hardened layer is too thin (z_h/b=0.5), it affects η only in the close-to-surface layer, whilst the critical point is still located at the maximum Hertz stress depth.

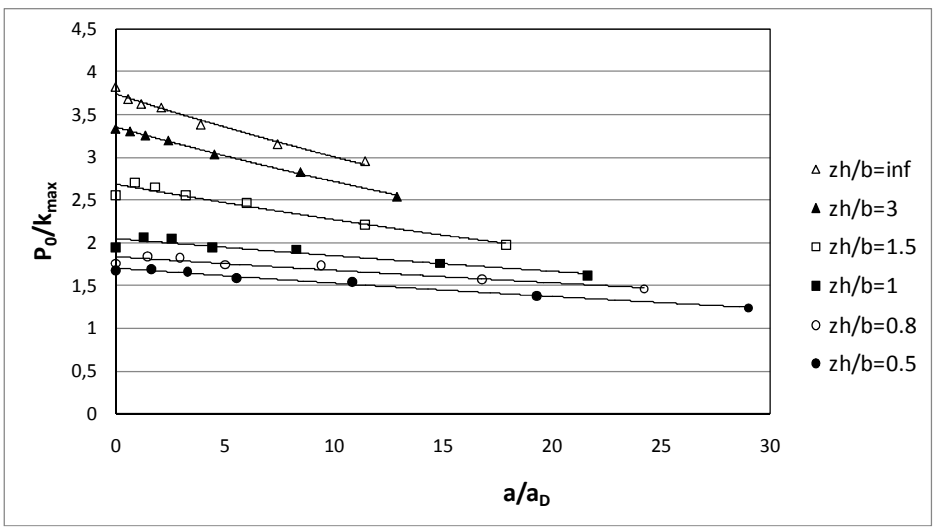

Fig.3: Dimensionless limit pressure vs defect size for different hardness profiles

In fig. 3, $p/\Delta\tau_0$ against a/a_D in frictionless contact is reported for the different hardness profiles considered, showing that the limit pressure decreases as the normalized defect dimension increases. Furthermore, as the hardness profile slope increases, the limit curves decrease. This diagram is of applicative usefulness: given the inclusion content (found by the extreme values statistics), and the loading condition, one can assess the lowest hardened depth which assures a sufficient fatigue strength.

4. Conclusions

A generalisation of a failure assessment diagram for rolling contact loading has been presented referring to components having hardness variable with depth. The diagram is constructed under the hypothesis that inherent defects are present in the components, behaving as equivalent short cracks and using the El-Haddad model to determine their propagation threshold; a relationship between applied stress intensity factor range and contact pressure, normalized respectively with respect to long crack fatigue growth threshold and contact pressure threshold in absence of defects, is then obtained. In the case of hardness variable with depth, all the material parameters were determined as a function of hardness itself. Several significant working cases, characterised by different defect size, contact surface friction and hardness profiles were simulated with this approach. Correspondent limit contact pressure values were obtained, highlighting the effect of the above parameters on them. All the results were finally collected in a graph of general validity, also expressed in a normalized form, which reports the limit contact pressure as a function of maximum expected inclusion size and hardness profile.

References

[1] Widmark M, Melander A. Effect of material, heat treatment, grinding and shot peening on contact fatigue life of carburised steels. *Int J of Fatigue* 1999; **21**: 309-327.
[2] Pariente IF, Guagliano M. Influence of Shot Peening Process on Contact Fatigue Behavior of Gears. *Mater and Manufactoring Processes* 2009; **24**: 1436-1441.
[3] Bormetti E, Donzella G, Mazzù A. Surface and subsurface cracks in rolling contact fatigue of hardened components. *Tribology Transactions* 2002; **45**; 3:274-283.
[4] Donzella G, Petrogalli C. A failure assessment diagram for components subjected to rolling contact loading. *Int Journal of Fatigue* 2010; **32**: 256-268.
[5] Auclair G. et al. (1997), Cleanliness Assessment : a Critical Review and a Real need to Predict Rolling Contact Fatigue Behaviour. In: *Proc 5th Int Symposium on Bearing Steels* 1997.
[6] Murakami Y. Metal Fatigue: Effects of Small Defects and Nonmetallic Inclusions. *Elsevier Science & Technology* 2002.
[7] El Haddad MH, Topper TH, Smith KN. Prediction of non propagating cracks. *Engineering fracture mechanics* 1979; **11**: 573-584.
[8] Yu MT, DuQuesnay DL, Topper T.H. Notch fatigue behaviour of SAE1045 steel. *Int Journal of Fatigue* 1988; **10**: 109-116.
[9] Dang Van K, Maitournam MH. Rolling contact in railways: modeling, simulation and damage prediction. *Fatigue and Fracture of Engineering Materials and Structures* 2003; **26**: 939-948.
[10] Desimone H, Bernasconi A, Beretta S. On the application of Dang Van criterion to rolling contact fatigue. *Wear* 2006; **260**: 567-572.
[11] Ciavarella M, Monno F, Demelio G. On the Dang Van fatigue limit in rolling contact fatigue. *Int Journal of Fatigue* 2006; **28**: 852-863.
[12] Atzori B, Meneghetti G, Susmel L. Material fatigue properties for assessing mechanical components weakened by notches and defects. *Fatigue and Fracture of Engineering Materials and Structures* 2005; **28**: 83-97.
[13] Roessle ML, Fatemi A. Strain-controlled fatigue properties of steels and some simple approximations. *Int Journal of Fatigue 2000*; **22**: 495-511.
[14] Kato M, Deng G, Inoue K, Takatsu N. Evaluation of the strength of carburized spur gear teeth based on fracture mechanics. *ISME Int. Journal Series C* 1993; **36**: 233-240.
[15] Mazzù A. A mode II weight function for subsurface cracks in a two-dimensional half-space. *Fatigue Fract Eng Mater Struct* 2002; **25**: 911-916.
[16] Sakae C, Ohkomori Y, Murakami Y. Mode II stress intensity factors for spalling cracks in backup roll. *Internal report*, Kyushu University 1999.